Biophysical tissue characterization of Ventricular Tachycardia substrate with Local Impedance mapping to predict critical sites

Júlia Aranyó MD[a,b], Daina Martínez-Falguera BSc[c,d], Víctor Bazan MD, PhD[a,b], Edgar Fadeuilhe MD[a], Albert Teis MD[a,c,e] Axel Sarrias MD[a], Oriol Rodríguez-Leor MD, PhD[a,e], Carolina Curiel BSc[f], Roger Villuendas MD[a,e], Antoni Bayés-Genís MD, PhD[a,b,c,e,g], Carolina Gálvez-Montón MD, PhD[a,c,e,†], Felipe Bisbal MD, PhD[a,b,c,e,†]

[a]Heart Institute (iCOR), Germans Trias i Pujol University Hospital, Badalona, Barcelona, Spain

[b]Department of Medicine, Autonomous University of Barcelona (UAB)

[c]ICREC Research Program, Germans Trias I Pujol Research Institute (IGTP), Badalona, Barcelona, Spain

[d]Department of Medicine University of Barcelona (UB), Spain

[e]CIBER Cardiovascular, Instituto de Salud Carlos III, Madrid, Spain

[f]Boston Scientific, Barcelona Delegation, Spain

[g]Department of Medicine, Can Ruti Campus, Autonomous University of Barcelona, Spain

[†]Dr Bisbal and Dr Gálvez-Montón share senior authorship.

Word count: 4678

Running title: LI mapping for VT substrate characterization

Correspondence Author:

Felipe Bisbal, MD, PhD, FESC

Germans Trias i Pujol University Hospital.

Carretera del Canyet s/n, 08916 Badalona, Spain

Phone: +34 93 497 83 98

Fax: +34 93 497 89 39

Email: f.bisbalvb@gmail.com

Carolina Gálvez-Montón, DVM, MSc, PhD

Germans Trias i Pujol Research Institute (IGTP)

Camí de les Escoles s/n, 08916 Badalona, Spain

Phone: +34 93 554 30 50 Ext. 6354

Fax. +34 93 497 86 54

Email: cgalvez@igtp.cat

Funding: This study was supported by research grants from Hospital Germans Trias I Pujol (programa de Talents 2021) and Investigator-Sponsored Research grant from Boston Scientific.

Conflicts of Interest: FB received speaker honoraria from Boston Scientific. Other authors have nothing to disclose.

Short tweet: Biophysical tissue characterization with Local impedance mapping identifies critical sites of VT circuit and provides new targets for ablation. #Epeeps #AblateVT

STRUCTURED ABSTRACT

Objectives: To test local impedance (LI)-based mapping to predict critical ventricular tachycardia (VT) components after myocardial infarction (MI).

Background: New tools are needed to improve VT substrate characterization and optimize outcomes. LI provides biophysical tissue characterization.

Methods: One-month after a non-reperfused anterior MI, endo-epicardial high-density electroanatomic mapping and endocardial LI mapping were performed in 23 Landrace Large X White pigs. LI thresholds were set using blood-pool (BP) value to define a 10Ω range: low (<BP-1Ω), intermediate (BP-1≤BP+9Ω), and high (normal) tissue resistance (>BP+9Ω).

Results: Low LI was detected in low voltage areas in 100% of cases but intermediate LI was found in both core (87%) and border zone (12.5%) voltage areas. Seventeen VTs were induced (VT isthmus identified in 9 animals). VT inducibility was associated with the size of intermediate LI area (OR 1.19 [1.0-1.4); p=0.039) and the presence of specific LI patterns: LI corridor (OR 15.0 [1.3-169.9]; p=0.029); LI gradient (OR 30.0 [2.1-421.1]; p=0.012), high LI heterogeneity (OR 21.7 [1.8-260.6]; p=0.015), and presence of ≥2 low LI regions (OR 11.3 [1.0-130.2]; p=0.053). Potential VT isthmuses were in areas of intermediate LI and colocalized to LI patterns associated with VT inducibility in all cases (LI corridors or LI gradient). Low LI regions did not actively participate in the VT circuit (0%).

Conclusions: LI mapping is feasible and may add useful characterization of the VT substrate. Specific LI patterns (i.e., corridors, gradients) were associated with VT inducibility and colocalized with the VT isthmus, thus representing a potential new target for ablation in substrate-based procedures.

KEYWORDS: local impedance, ventricular tachycardia, catheter ablation, tissue characterization

CONDENSED ABSTRACT

New tools are needed to improve outcomes of ventricular tachycardia (VT) ablation. Local impedance (LI) is based on biophysical tissue properties. We tested LI-based mapping to predict critical VT components in a post-myocardial infarction swine model. VT inducibility was associated with intermediate LI area (OR 1.19; p=0.039) and specific LI patterns (LI corridor [OR 15; p=0.029], LI gradient [OR 30; p=0.012], and high LI heterogeneity [OR 22; p=0.015]). Potential VT isthmuses were in intermediate LI areas and colocalize with LI patterns associated with VT inducibility (LI corridors or gradients) in all cases, thus representing a potential new target for ablation in substrate-based procedures.

ABRREVIATION LIST

MI: myocardial infarction

LI: local impedance

EGM: electrogram

VT: ventricular tachycardia

LAVA: local abnormal ventricular activity

LP: late potential

INTRODUCTION

Despite advances in mapping and ablation technologies, catheter ablation of scar-related ventricular tachycardia (VT) still achieves only moderate clinical efficacy, with a substantial recurrence rate.[1,2] The contemporary approach to VT aims to identify and eliminate the critical sites of myocardial scar serving as VT isthmuses. Activation and entrainment mapping during tachycardia were the initial strategies to identify critical components of the VT circuit, but are limited to inducible, hemodynamically tolerated VTs. Substrate-based approaches were developed to characterize arrhythmogenic substrate during sinus or paced rhythms.[3,4,5,6] Low voltage areas and electrograms with delayed components or abnormal response to extrastimuli have been considered the most relevant sites amenable to ablation, but may not be critical for re-entrant activity. Moreover, critical sites of the VT circuit do not consistently exhibit abnormal electrograms or voltage in sinus rhythm; consistency of definitions of abnormal signal or voltage may vary depending on wavefront direction or electrodes/catheter configuration.[7] Thus, identification of critical components of the VT circuit remains challenging and extensive ablation is often required to achieve non-inducibility.[8] New tools and strategies are still needed to improve tissue characterization and mechanistic understanding of the VT circuits to optimize ablation and improve outcomes.

Impedance is defined as a material's opposition to the flow of electric current, influenced by its resistance as well as inductive and capacitive reactance.[9] Local impedance (LI) is a direct measurement of the resistive load and has been shown to be a reliable tool to assess tissue composition.[10,11] DirectSense™ technology (Boston Scientific, Massachusetts, MA), a commercially available tool, allows for real-time LI measurement. Preclinical data showed LI to be a highly sensitive tool to distinguish tissues with dissimilar resistivity, as well as to evaluate lesion formation in real time.[12,13,14,15,16,17] Differences in tissue composition lead to differences in LI values. The biological mechanism leading to a lower LI of fibrotic tissue is not fully

understood, although a plausible explanation is the greater proportion of extracellular matrix and the aqueous amorphous phase of the infarcted myocardium.[18] Ischemic scars are complex and highly heterogeneous with variable proportions of collagen, fibroblasts, viable cardiomyocytes, and adipose tissue; hence, different LI values are present within the scar.[19, 20]

We sought to assess the usefulness of a LI-based biophysical characterization of the ischemic VT substrate and its capability to predict critical components of the circuit for VT inducibility.

METHODS

Swine myocardial infarction model

Twenty-eight Landrace X Large white pigs (30-35kg; 50% females) were submitted to a non-reperfused myocardial infarction (MI), as previously described.[21] Extended methods are available in the Supplementary Material. Briefly, MI was induced by percutaneous selective coil embolization (VortX-18 Diamond 3 mm/3.3 mm coil, Boston Scientific/Target, Natick, MA, USA) of the left anterior descending (LAD) coronary artery after the first diagonal branch, under general anaesthesia.

Complete thrombotic occlusion was confirmed by persistent ST-segment elevation and by repeating coronary angiography 10 min after coil implantation (TIMI flow score =0). Animals were recovered and survived for 1 month following the MI induction procedure.

Electroanatomic mapping

Animals underwent invasive electrophysiology study and high-density electroanatomic mapping (HDM) at 1-month post-MI. Detailed procedure protocol is provided in Supplementary Material. A 4-pole catheter was placed at the right ventricular apex. Endo-epicardial left ventricular HDM was performed using the Rhythmia HDx 3D mapping system and a 64-pole basket catheter (Intellamap Orion, Boston Scientific, Massachusetts, USA). Retrograde aortic access was used for the endocardium and sub-xiphoid puncture for the

epicardium. HDM was performed at a paced cycle length of 400ms with 1 extrastimuli 20ms above the ventricular effective refractory period. Filling threshold was ≤2 mm in regions of low bipolar voltage and ≤10 mm elsewhere; interpolation between points ≤2 mm was required in all cases. Bipolar electrograms were recorded with bandpass filters of 30 to 300Hz.

All electroanatomic maps were analyzed offline with the Rhythmia system. Standard peak-to-peak bipolar voltage thresholds were used (0.5 and 1.5mV) to define core, border zone (BZ) and healthy tissue. Core and BZ voltage regions were quantified using the mapping system's surface area measurement utility. Voltage channels were identified by dynamic readjustment of voltage cut-offs (voltage scanning).[22] Complete voltage channel was defined as a corridor of continuous normal or BZ voltage surrounded by 2 dense (core) scar areas or anatomical barrier, and connected to normal myocardium by at least two sites[22] The Lumipoint™ module was used to rapidly highlight and re-annotate –if necessary– slow and delayed conduction, including the number of deceleration zones (DZ), defined as regions with >3 of 8 isochrones within 1cm comprising the entire ventricular activation window. Local abnormal ventricular activities (LAVA), late potentials (LP) and DZ were tagged and co-registered with LI and VT maps. The definition of LP and LAVA was based on activation timing with respect to the QRS complex.

Local Impedance mapping

Catheter-based LI technology generates a non-stimulatory alternating current (5.0μA, 14.5KHz) from the catheter tip to the proximal ring creating a local electric field. Changes in this electric field, caused by different tissue-resistivity or catheter-tissue proximity, are sensed by three mini-electrodes embedded in the catheter tip (Supplemental figure S1). A point-by-point LI map was created in sinus rhythm using the Intellanav MiFi OI™ ablation catheter (Boston Scientific, Massachusetts, USA) via retrograde aortic access. First, baseline blood pool (BP) LI was recorded as a reference value while maintaining the catheter floating in the left ventricle

cavity. Next, the 3D LI map was created by recording the LI value (measured in ohms, Ω) at each endocardial point, manually annotating it on a local activation time (LAT) map as activation time in milliseconds (Supplemental figure S2).

Endocardial LI was acquired with a minimum filling threshold of 6mm (the assumed field of view of LI).[12] When possible, increased point density was attempted. Catheter-tissue contact was ensured by tactile feedback, electrogram amplitude, fluoroscopy, and LI stability. Since LI values were usually above BP and values variations within the scar did not usually exceed 10-ohm, LI thresholds were set using baseline BP as the inferior cut-off and a scale range of 10 ohm to define low (<BP-1Ω), intermediate (>BP-1 and ≤BP+9Ω), and high tissue resistance (>BP+9Ω). High tissue resistance was considered normal tissue, while low and intermediate were considered abnormal. The size of different LI types was quantified using the mapping system's surface area measurement software and outlines were co-registered with voltage maps. Overlap between abnormal (low or intermediate) LI and voltage subtype (core, BZ, or healthy tissue) was categorized based on the predominant voltage amplitude in the overlapped area. Previous investigation demonstrated that LI of the myocardium is significantly greater than BP.[12] We explored the relationship between BP and tissue LI by incorporating the LI ratio (LIR=Tissue LI/BP LI). Similar to voltage channels, LI corridors were explored by step-by-step 1 Ohm adjustment of LI cut-offs (maintaining the 10 Ohm range) until the upper cut-off reached the BP. LI corridor was defined as a higher resistivity corridor connecting 2 healthy areas and surrounded by lower LI tissue. Following LI scanning, an "iso-impedance" map was displayed using LI isochrones of 1 Ohm. Although LI values were not activation points and therefore the concept of isochrones would be inappropriate, the iso-impedance map was performed to explore tissue heterogeneity, crowding, and gradients. Significant LI gradient was defined as ≥3 isochrones within a 1 cm radius (Figure 1). LI heterogeneity was categorized as high or low depending on the presence and distribution of complete (LI ≤BP+9) or incomplete abnormal LI range of the scar (Figure 1).

Ventricular Tachycardia inducibility and mapping

Following HDM and LI mapping, induction of VT was attempted. Programmed ventricular stimulation protocol was performed from right and left ventricle with S1 trains of 400, 350, and 300 ms up to S5 coupled at 20 ms above the ventricular effective refractory period. If an hemodynamically tolerated sustained monomorphic VT was induced, a high-density activation map was attempted. Data acquisition during VT was automatic, using the following criteria for beat acceptance: tachycardia cycle length stability ±5ms, 12-lead ECG morphology match, stability of relative timing of reference electrograms, and respiration gating; afterwards, all electrograms were reviewed offline. Activation maps were accepted if they accounted for at least 80% of tachycardia cycle length. Re-entrant mechanism was defined based on the activation map. Entrainment was not performed due to high risk of VT acceleration/VF or termination. Animals were euthanized by administering a sodium thiopental overdose (200 mg/kg) at the end of the mapping procedure. Corregistration between electroanatomical, LI and VT activation maps was performed off-line (Supplemental figure S3).

Ethical implications

The research protocol was approved by the Animal Experimentation Unit Ethics Committee of the Germans Trias i Pujol Health Research Institute (IGTP) and by the competent governmental authority (Generalitat de Catalunya; Code: CEA-OH/11208/1), and complies with all guidelines concerning the use of animals in research and teaching as defined by the Guide for the Care and Use of Laboratory Animals (*National Research Council (US) Committee for the Update of the Guide for the Care and Use of Laboratory Animals. Guide for the care and use of laboratory animals. 8th ed. Washington (DC): National Academies Press (US); 2011*.). Research was performed at the Comparative Medicine and Bioimage Centre of Catalonia, Spain (CMCiB).

Statistical Analysis

Statistical analyses were performed with SPSS (19.0.1 version, SPSS, Inc. Chicago, IL, USA) software. Continuous variables were expressed as mean ± SD or median with interquartile range, as appropriate; categorical variables were expressed as relative and percentages. Continuous variables were compared with either Student t tests or non-parametric Mann-Whitney U tests; categorical variables were compared using Chi-square or Fisher exact test, as needed. Values of $p<0.05$ were considered significant.

RESULTS

Twenty-eight pigs underwent the MI induction procedure, with acute mortality of 18% (n=5) due to ventricular fibrillation. The remaining 23 animals survived the 1-month post-operative period.

Electroanatomic and Local Impedance mapping

Endocardial and epicardial HDM were performed in 23 (100%; 2222±574 points) and 19 (82.6%; 5149±1561 points) animals, respectively. In all animals, LAD occlusion resulted in an anterior wall infarction with an extensive area of low endocardial bipolar voltage (median area ≤1.5mv was 22.1[14.2-29.1]cm2 and ≤0.5mV, 17.2[10.8-21.5]cm2). Low epicardial bipolar voltage (median area ≤0.5mV, 8.1[5.9-9.5]cm2) was observed in 17 (89.5%) of the animals in which epicardial HDM was performed.

The LI endocardial mapping (78± 25 points), performed in all animals, had a median BP LI of 78[73-81]Ω. The median [IQR] filling threshold of LI maps was 3 [3.0-5.0]. Median [IQR] LIR and LI were 0.95[0.94-0.97] and 73.7[68.4-76.4]Ω for low, 1.05[1.03-1.07] and 81.8[75.5-83.4]Ω for intermediate, and 1.36[1.31-1.41] and 113.2[98.6-119.5]Ω for high resistivity tissue, respectively. The median area of the abnormal, low, and intermediate LI was 21.9[11.1-25.3] cm2, 4.6[0-7.8] cm2, and 14.3[4.3-18.9] cm2, respectively. Colocalization between abnormal voltage and LI was not linear. Low LI was consistently detected in core voltage areas in 100% of cases, but intermediate LI colocalized with both core (87%) and BZ areas (13%).

None of the animals exhibited voltage corridor using the standard cut-off values; after voltage scanning, a voltage corridor could be identified in ten cases (43.5%). LI corridors were identified in 13 (56%) cases (6 [26%] with standard cut-offs and 7 [30%] after LI scanning). Five (55.6%) voltage channels overlapped with a corresponding LI corridor. LI corridors were protected by two (87.5%) or three (12.5%) regions of low LI.

High LI heterogeneity was observed in 13 (56%) of the animals; the remaining ten animals presented only one or two predominant LI values (low LI heterogeneity). Sixteen animals (69%) had a significant LI gradient, with a median of 2[1-2] per animal (23.5%, 58.8% and 17.6% presented 1, 2 and 3 LI gradient regions, respectively).

Abnormal electrograms (LAVA or LP) were found in 18 (78.2%) and 13 (68.4%) animals at the endocardium and epicardium, respectively. Most abnormal endocardial EGMs (91%) were registered at intermediate LI areas, with only 9% occurring in low LI regions. Likewise, the regions of abnormal epicardial electrograms overlapped with endocardial intermediate LI in 12 (92%) of the animals and only 1 overlapped with a low LI; and 68.4% of areas of intermediate LI colocalized with abnormal potentials (LAVA) at the epicardial surface.

Fourteen (61%) animals presented at least one DZ (1[0-2] DZ/animal), which colocalized with intermediate LI regions in all cases (median LI in DZ of 80[76-86]Ω) and with a LI corridor or a LI gradient in 64.2% (9/14).

VT inducibility: LI, voltage, and VT mapping

A total of 20 sustained monomorphic VTs were induced in 17 animals (mean cycle length 210± 37 msec), requiring inotropic support in all cases. Activation mapping (4725±3343 points) revealed a re-entrant mechanism in all cases.

Identification of the presumptive critical isthmus was possible in 9 cases (53%): 8 endocardial and 1 epicardial. The median LI at critical site was 82 [78.8-85.5]Ω (intermediate LI in all cases)

and median LI/BP ratio was 1.08 [1.05-1.12]. Diastolic components of the VT colocalized with low voltage (core, <0.5mV) and intermediate LI sites in all cases. All VT isthmuses colocalized to LI patterns associated with VT inducibility in all cases: LI corridor in 77.8% (n=7) and LI gradient in 55.5% (n=5), as shown in Figures 3 and 4. Low resistivity tissue did not actively participate in the VT circuit but rather acted as tissue boundary protecting the critical diastolic pathway in all cases.

Table 1 summarizes differences in voltage and LI mapping between animals with inducible and non-inducible VT. Compared to animals with non-inducible VT, those with induced or spontaneous VT had larger scars (voltage area <1.5mV 22.8 [20.6-30.0] vs 13.0 [2.2-19.8]cm2, p=0.021), with larger core area (voltage area <0.5mV 18.9 [15.4–25.0] vs. 10.2 [0-14.9]cm2, p=0.025). Low voltage (<0.5mV) area was associated with VT inducibility (1.143 [1.038-1.260]; p=007). The size of core area (1.177 [1.014-1.367]; p=0.032) and of BZ (2.512 [1.037-6.084]; p=0.041) associated with VT induction.

Animals with induced VT had larger area of abnormal LI (22.6 [16.1-27.0] vs 8.1 [0-16.5]cm2, p=0.030), with more extensive intermediate LI zones (16.1 [9.6-23.4] vs. 2.1 [0-7.9]cm2, p=0.021) but without differences in low LI area (5.1 [2.2-6.9] vs. 2.1 [0-10.4]cm2, p=0.780). The area of intermediate LI, but not low LI, was associated with increased probability of inducible VT (OR 1.19 [1.01-1.40) for each cm2; p=0.039). Animals with inducible VT had higher prevalence of LI corridors (70.6 vs. 16.7%, p=0.014), LI gradient (82.3 vs 33.3%, p=0.011), high LI heterogeneity (70.6 vs. 16.7%, p=0.014), and low LI regions (2.1±0.7 vs. 0.8±0.4; p=0.002) compared to those with non-inducible VT. These specific LI distribution patterns significantly increased the likelihood of inducible VT: LI corridor (OR 15.00 [1.33-169.87]; p=0.029), LI gradient (OR 30.00 [2.14-421.12], p=0.012), high LI heterogeneity (OR 21.67 [1.80-260.57]; p=0.015), and presence of ≥2 low LI regions (OR 11.25 [1.00-130.22]; p=0.053) (Table 2).

There were more DZ areas in the inducible compared to non-inducible animals (2 [1-3] vs. 0 [0-1], p=0.033), without differences in presence of voltage corridors (53% vs. 17%, p=0.149). DZ (OR 5.20 [0.71-37.89]; p=0.104) and voltage corridors (OR 2.57 [0.36-18.32]; p=0.346) were not associated with VT inducibility.

Discussion

The present study has three major findings: 1) LI-based biophysical tissue characterization of ventricular ischemic scar is feasible and adds useful information to predict potential critical components; 2) Potential VT isthmuses were consistently located in intermediate LI regions regardless of voltage amplitude; and 3) The presence of specific LI distribution patterns (i.e. corridors, LI gradients, tissue heterogeneity) was associated with VT inducibility and colocalized with presumptive VT isthmuses in all cases (central illustration).

To the best of our knowledge, this is the first study providing feasibility data on LI mapping of ischemic VT substrate and showing the added value of LI in predicting VT inducibility and location of critical sites of the VT circuit. The rationale for substrate-based mapping strategies relies on identification of viable myocyte bundles embedded within the scar and that have a delayed activation during sinus or paced rhythm. The absolute endocardial voltage value and additional electrogram characteristics (late, split, or fragmented EGMs) may be insufficient to precisely identify sites harbouring myocardial re-entry, as these characteristics may be influenced by multiple circumstances, such as wavefront direction, preferential fibre orientation, catheter-tissue orientation, isthmus and circuit structure, etc.[4] LI is a biophysical property highly influenced by tissue structure and properties and independent on the aforementioned factors.[23] In our study, although large, homogeneous low voltage scar areas were identified in all animals, LI patterns were significantly heterogeneous. Endocardial voltage mapping had a mean of >2000 points, which make the presence of false low voltage

zones very unlikely. We found that low resistivity tissue (low LI) was consistently found in dense, very-low voltage areas; however, intermediate LI tissue could be found in both voltage core and BZ areas, allowing for further discrimination of different tissue compositions and refinement of the substrate definition.

Ventricular tachycardia was more frequently induced in animals with ≥2 regions of low LI. Low resistivity tissue predominantly acted as tissue boundary and did not actively participate as a critical VT isthmus, instead acting as a fixed barrier protecting diastolic pathway. VT isthmuses were found in intermediate LI regions in all cases. Previous studies have evaluated the concept of re-entrant circuits delimited by anatomic barriers using voltage criteria, with controversial results. There is a general consensus, however, that voltage channels are not specific markers of VT isthmuses. [24] LI is predominantly determined by cellular features (i.e. intracellular and cell membrane contents) but also by architectural aspects (i.e. cellular size, cellular arrangement, and wall thickness). In fact, the use of LI as a tool to characterize different tissues, including identification of malignant tissue or characterization of different components of the same organ (i.e. fundus vs. antrum), is not new. [25] LI mapping in the heart could add valuable structural tissue information to further characterize scar composition and identify potential critical sites and boundaries of VT. Pathological evaluation would provide insightful data on the underlying tissue composition of different LI categories.

The novelty of the present study is the observation that specific LI patterns (corridors and gradients) are strongly associated with VT inducibility, suggesting that distribution of LI within the scar may be relevant to VT circuits. We hypothesize that regions with LI gradient (significant isoimpedance crowding) and LI corridor may represent heterogeneous tissue composition with abnormal conduction properties. Areas exhibiting abrupt changes of LI may reflect the biophysical manifestation of abrupt tissue changes hampering wavefront

propagation and favouring conduction block. This is particularly relevant in the LI corridors, in which low LI regions protect intermediate LI zones corresponding to VT protected isthmus.

Ischemic scars and VT isthmuses are three-dimensional structures. Despite comprehensive high-density mapping, some parts of the tachycardia circuit may remain elusive at the endocardial surface. We observed that epicardial sites with abnormal conduction properties colocalized with areas of intermediate endocardial LI, suggesting that LI may act as a surrogate of transmurality and predict remote substrate. However, the benefit of LI mapping over traditional strategies to identify intramural/epicardial substrate (endocardial unipolar voltage mapping, cardiac magnetic resonance, etc.) should be further investigated.

Our work builds on the quest to identify culprit substrate for VT maintenance and provides potential new ablation targets for substrate-based procedures regardless of the underlying rhythm. Further research and technical developments to validate and automatize LI acquisition and mapping are key to allow for clinical implementation of this new technique. The development of an automatic “high density LI mapping” approach could offer an opportunity to refine the characterization of the VT substrate and to consolidate new ablation targets. New normalized/percentage LI thresholds need to be evaluated in future studies.

Limitations

Non-reperfused MI swine model was used in the study to resemble the most frequent clinical scenario of VT in ischemic cardiomyopathy. The number of hemodynamically tolerated VTs was rather small. Confirmation of VT isthmuses by entrainment mapping was not performed and thus, VT isthmuses were considered presumptive. LI data was acquired with non-contact force catheters, but strict criteria of catheter-tissue contact were applied (fluoroscopy, tactile feedback, electrogram amplitude, and LI stability). Whether LI maps acquired with contact-force sensing catheters would differ from those obtained in the study requires further

investigation. Catheter-tissue orientation was not assessed; however, previous data suggest no significant variations.[12] LI thresholds were set based on observational data from the study and should only apply to post-MI scar. Only one LI map was obtained per animal; further studies are required to assess the consistency and reproducibility of this technique. The field of view of LI is not yet fully understood and hence, the influence of point density on LI maps should be further evaluated; nevertheless, the highest, feasible LI point density was attempted in our study. The underlying pathology of the tissue at different LI categories was not evaluated (example of one animal is shown in supplemental figure S4). Given the limitations of this proof of concept study, results must be considered hypothesis-generating and require further confirmatory studies.

Conclusions

Local impedance mapping is feasible and may add useful tissue characterization of the VT substrate. Specific LI patterns (i.e., corridors, gradients) were associated with VT inducibility and consistently colocalized with the VT isthmus, thus representing a potential new target for ablation in substrate-based procedures.

CLINICAL PERSPECTIVES

Competency in medical knowledge

This study provides evidence on the feasibility and usefulness of local impedance (LI) based mapping to characterize VT substrate. Specific LI patterns predicted the location of critical components of scar-related VT; thus, LI mapping may provide potential new targets for ablation in substrate-based procedures.

Translational Outlook

Further research is required to define LI thresholds and patterns in other VT substrates including non-ischemic cardiomyopathy, non-reperfused myocardial infarction, etc. Clinical evaluation in humans is crucial to evaluate the reproducibility of the findings and assess the potential clinical benefit of LI mapping. Development of an automatized “high density LI mapping” could help to refine tissue characterization of VT substrate and potentially provide new targets for ablation.

ACKNOWLEDGMENTS

We are grateful to the Center of Comparative Medicine and Bioimaging of Catalonia (CMCiB) for their contribution in the animal model execution.

REFERENCES

1. Delacrétaz E, Brenner R, Schaumann A, et al. Catheter ablation of stable ventricular tachycardia before defibrillator implantation in patients with coronary heart disease (VTACH): An on-treatment analysis. *J Cardiovasc Electrophysiol*. 2013. doi:10.1111/jce.12073

2. Stevenson WG, Wilber DJ, Natale A, et al. Irrigated radiofrequency catheter ablation guided by electroanatomic mapping for recurrent ventricular tachycardia after myocardial infarction the multicenter thermocool ventricular tachycardia ablation trial. *Circulation*. 2008;118(25):2773-2782. doi:10.1161/CIRCULATIONAHA.108.788604

3. Bogun F, Bender B, Li YG, et al. Analysis during sinus rhythm of critical sites in reentry circuits of postinfarction ventricular tachycardia. *J Interv Card Electrophysiol*. 2002. doi:10.1023/A:1020832502838

4. Josephson ME, Anter E. Substrate Mapping for Ventricular Tachycardia. *JACC Clin Electrophysiol*. 2015. doi:10.1016/j.jacep.2015.09.001

5. Reddy VY, Neuzil P, Taborsky M, Ruskin JN. Short-term results of substrate mapping and radiofrequency ablation of ischemic ventricular tachycardia using a saline-irrigated catheter. *J Am Coll Cardiol*. 2003. doi:10.1016/S0735-1097(03)00492-3

6. Soejima K, Suzuki M, Maisel WH, et al. Catheter Ablation in Patients With Multiple and Unstable Ventricular Tachycardias After Myocardial Infarction. *Circulation*. 2001. doi:10.1161/hc3101.093764

7. Anter E. Limitations and Pitfalls of Substrate Mapping for Ventricular Tachycardia. *JACC Clin Electrophysiol*. 2021. doi:10.1016/j.jacep.2021.02.007

8. Di Biase L, Santangeli P, Burkhardt DJ, et al. Endo-epicardial homogenization of the scar versus limited substrate ablation for the treatment of electrical storms in patients with ischemic cardiomyopathy. *J Am Coll Cardiol*. 2012. doi:10.1016/j.jacc.2012.03.044

9. Slurzburg, Morris and Osterheld, William. Essentials of electricity for radio and television. New York: McGraw-Hill Book Company, 1950. 533 p. $4.00. *Sci Educ*. 1950. doi:10.1002/sce.3730340553

10. Jacobson JT, Hutchinson MD, Cooper JM, Woo YJ, Shandler RS, Callans DJ. Tissue-specific variability in human epicardial impedance. *J Cardiovasc Electrophysiol*. 2011. doi:10.1111/j.1540-8167.2010.01929.x

11. Fallert MA, Mirotznik MS, Downing SW, et al. Myocardial electrical impedance mapping of ischemic sheep hearts and healing aneurysms. *Circulation*. 1993. doi:10.1161/01.CIR.87.1.199

12. Sulkin MS, Laughner JI, Hilbert S, et al. Novel Measure of Local Impedance Predicts Catheter-Tissue Contact and Lesion Formation. *Circ Arrhythmia Electrophysiol*. 2018. doi:10.1161/CIRCEP.117.005831

13. Martin CA, Martin R, Gajendragadkar PR, et al. First clinical use of novel ablation catheter incorporating local impedance data. *J Cardiovasc Electrophysiol*. 2018. doi:10.1111/jce.13654

14. Sasaki T, Nakamura K, Inoue M, et al. Optimal local impedance drops for an effective radiofrequency ablation during cavo-tricuspid isthmus ablation. *J Arrhythmia*. 2020. doi:10.1002/joa3.12403

15. Münkler P, Gunawardene MA, Jungen C, et al. Local impedance guides catheter ablation in patients with ventricular tachycardia. *J Cardiovasc Electrophysiol*. 2020. doi:10.1111/jce.14269

16. Piorkowski C, Sih H, Sommer P, et al. First in human validation of impedance-based catheter tip-to-tissue contact assessment in the left atrium. *J Cardiovasc Electrophysiol*. 2009. doi:10.1111/j.1540-8167.2009.01552.

17. Garrott K, Laughner J, Gutbrod S, et al. Combined local impedance and contact force for radiofrequency ablation assessment. Heart Rhythm. 2020 Aug;17(8):1371-1380

18. Gaspar T, Sih H, Hindricks G, et al. Use of electrical coupling information in AF catheter ablation: A prospective randomized pilot study. *Hear Rhythm*. 2013. doi:10.1016/j.hrthm.2012.10.010

19. Cinca J, Warren M, Rodríguez-Sinovas A, et al. Passive transmission of ischemic ST segment changes in low electrical resistance myocardial infarct scar in the pig. *Cardiovasc Res*. 1998. doi:10.1016/S0008-6363(98)00145-X

20. Barkagan M, Leshem E, Shapira-Daniels A, et al. Histopathological Characterization of Radiofrequency Ablation in Ventricular Scar Tissue. *JACC Clin Electrophysiol*. 2019. doi:10.1016/j.jacep.2019.05.011

21. Martínez-Falguera D, Fadeuilhe E, Teis A, et al. Myocardial Infarction by Percutaneous Embolization Coil Deployment in a Swine Model. *J Vis Exp*. 2021. doi:10.3791/63172

22. Arenal A, Del Castillo S, Gonzalez-Torrecilla E, et al. Tachycardia-related channel in the scar tissue in patients with sustained monomorphic ventricular tachycardias: Influence of the voltage scar definition. *Circulation*. 2004. doi:10.1161/01.CIR.0000145544.35565.47

23. Amorós-Figueras G, Jorge E, Alonso-Martin C, et al. Endocardial infarct scar recognition by myocardial electrical impedance is not influenced by changes in cardiac activation sequence. Heart Rhythm. 2018. doi:10.1016/j.hrthm.2017.11.031

24. Mountantonakis SE, Park RE, Frankel DS, et al. Relationship between voltage map “channels” and the location of critical isthmus sites in patients with post-infarction cardiomyopathy and ventricular tachycardia. *J Am Coll Cardiol*. 2013. doi:10.1016/j.jacc.2013.02.031

25. Chiang S, Eschbach M, Knapp R, et al. Electrical impedance characterization of in vivo porcine tissue using machine learning. *J Electr Bioimpedance*. 2021. doi:10.2478/JOEB-2021-0005

FIGURE LEGENDS

Figure 1. LI patterns associated with VT inducibility. The upper panel shows Local impedance (LI) maps from 3 animals with inducible ventricular tachycardia. **Panel A**. Corridor of intermediate LI between two areas of low LI and connecting with healthier myocardium (higher LI). **Panel B.** Example of heterogeneous scar with 2 areas of significant LI gradient (isoimpedancemap). **Panel C.** Extensive scar with presence of both LI corridor and significant LI gradient. The lower panel shows LI heterogeneity patterns. **Panel D**. Extensive scar with abnormal but homogeneous resistivity with one predominant LI (low LI heterogeneity) in a pig with non-inducible ventricular tachycardia (VT). **Panel E.** Scar exhibiting high LI heterogeneity in an animal with inducible VT.

Figure 2. VT isthmus and LI corridor. Example of a pig with extensive anterior infarction and inducible VT. The endocardial bipolar voltage map shows an extensive low (<0.5mV) voltage area (**Panel A**) without a clear voltage channel (**panel B**). Despite homogeneous voltage <0.5mV, high tissue heterogeneity was found in the LI map with a corridor of intermediate LI between two areas of low LI (**Panel C**). The activation map of induced VT (**Panel D**) demonstrated colocalization of thediastolic components (presumptive VT isthmus) with the LI corridor but in a homogeneous, low-voltage area (<0.5mV).

VT: ventricular tachycardia; BP: blood pool; p: pressumptive

Figure 3. VT isthmus and LI gradient. The endocardial bipolar voltage map shows an extensive low (<0.5mV) voltage area located at the left ventricular apex (**panel A**) with a potential voltage channel at the apex (**panel B**). The LI map performed in sinus rhythm showed a significant LI gradient (intermediate LI range) between two areas of lower LI (**panel C**). The activation map of the induced VT showed a presumptive isthmus that colocalized with the LI gradient region but not with the voltage channel.

BP: blood pool

Central Illustration. Local impedance mapping for VT substrate characterization. Local impedance (LI) based mapping was tested to predict critical VT components in a post-myocardial infarction swine model. Voltage and LI mapping, as well as induction protocol and activation mapping were performed. VT inducibility was associated with the size of intermediate LI area and with specific LI distribution patterns (LI corridor, LI gradient and high LI heterogeneity). Critical VT isthmuses were in intermediate LI areas and colocalize with proarrhythmic LI patterns in all cases.

Table 1. Voltage and Local impedance parameters in non-inducible vs. inducible group.

	Non-inducible VT (n=6)	Inducible VT (n=17)	P value
Voltage and activation data			
Area <0.5mV, cm2	10.2 [0-14.9]	18.9 [15.4–25.0]	**0.025**
Area <0.1mV, cm2	3.2 [0.5-7.2]	5.8 [3.5-8.1]	0.208
Area 0.5-1.5mV, cm2	3.1 [2.1-4.9]	4.9 [3.1-6.4]	0.151
Area <1.5mV, cm2	13.0 [2.2-19.8]	22.8 [20.6-30.0]	**0.021**
Voltage corridor (standard cut-off)	0	0	-
Voltage corridor (scanning), n (%)	1 (17)	9 (53)	0.149
DZ (number)	0 [0-1]	2 [1-3]	**0.033**
LI data			
LI Blood pool, Ω	76.0 [72.0-78,3]	79.5 [76.5-82.7]	0.077
Low LI area, cm2	2.1 [0-10.4]	5.1 [2.2-6.9]	0.780
Intermediate LI area, cm2	2.1 [0-7.9]	16.1 [9.6-23.4]	**0.021**
Total abnormal LI area, cm2	8.1 [0-16.5]	22.6 [16.1-27.0]	**0.030**
High LI heterogeneity pattern	1 (16.7)	12 (70.6)	**0.014**
LI corridor (standard cut-off)	0	6 (35.2)	0.123
LI corridor (standard or adjusted cut-off)	1 (16.7)	12 (70.6)	**0.014**
Low LI zones (standard cut-off)	1 [0-1]	2 [1-2]	0.054
Low LI zones (standard cut-off or adjusted cut-off)	1 [0-1]	2 [1-3]	**0.040**
Significant LI gradient zones	2 (33.3)	14 (82.3)	**0.011**

VT: ventricular tachycardia; DZ: deceleration zone; LI: local impedance

Table 2. Predictors of VT inducibility.

	OR	P value
Voltage and activation data		
Core voltage area (<0.5mV), cm2	1.177 (1.014-1.367)	**0.032**
Core voltage area (<0.1mV), cm2	1.351 (0.943-1.936)	0.101
Intermediate voltage area (0.5-1.5mV), cm2	2.512 (1.037-6.084)	**0.041**
Abnormal voltage area (<1.5mV), cm2	1.177 (1.023-1.355)	**0.023**
Voltage corridor (scanning)	2.571 (0.361-18.326)	0.346
DZ	5.200 (0.714-37.895)	0.104
Local Impedance data		
Low LI area, cm2	1.072 (0.865-1.330)	0.525
Intermediate LI area, cm2	1.190 (1.009-1.403)	**0.039**
Total abnormal LI area, cm2	1.166 (1.016-1.337)	**0.029**
LI corridor	15.000 (1.325-169.870)	**0.029**
Significant LI gradient	30.000 (2.137-421.117)	**0.012**
High LI heterogeneity	21.667 (1.802-260.574)	**0.015**
Presence of ≥2 regions of low LI	11.25 (0.972-130.221)	**0.053**

VT: ventricular tachycardia; DZ: deceleration zone; LI: local impedance

1 **FIGURES**

2 **Figure 1**

3

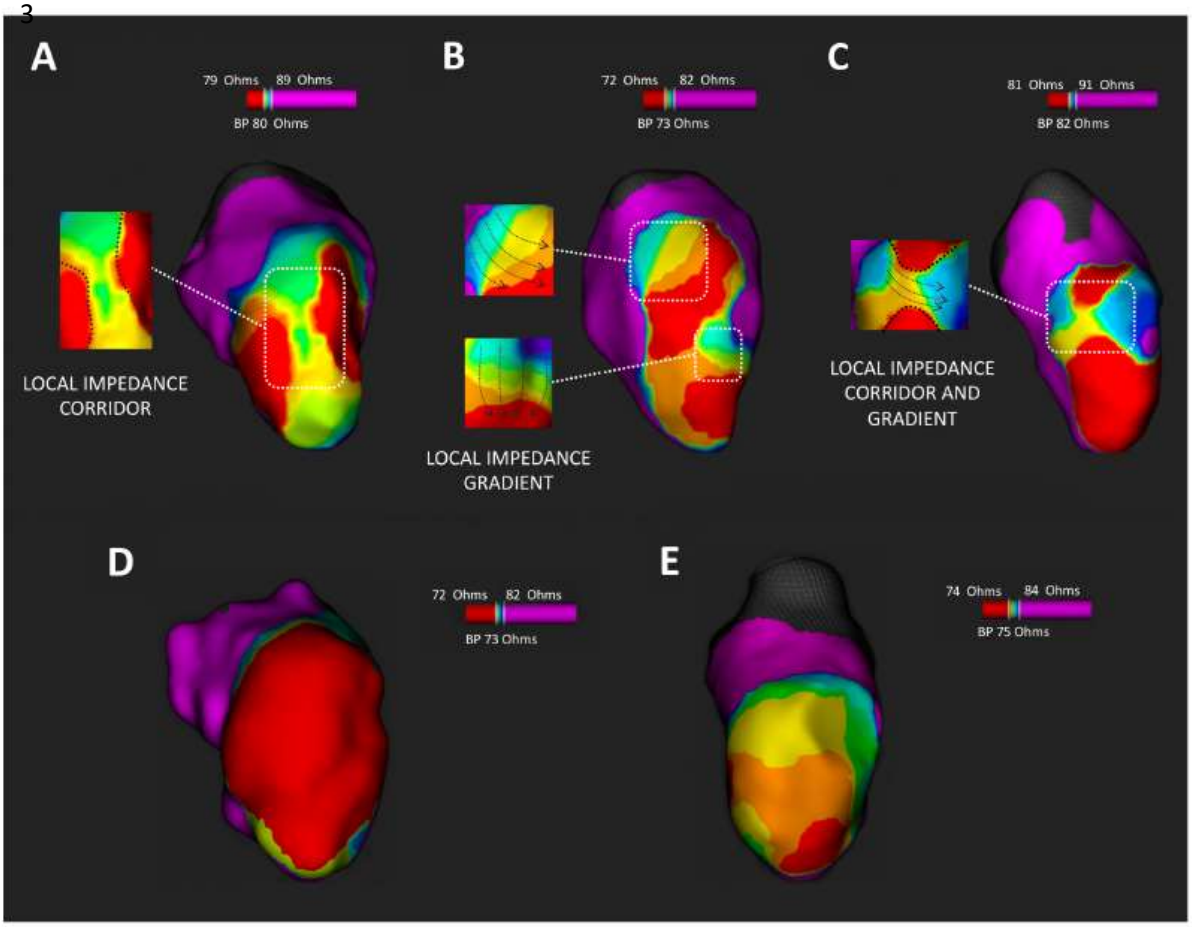

Figure 2

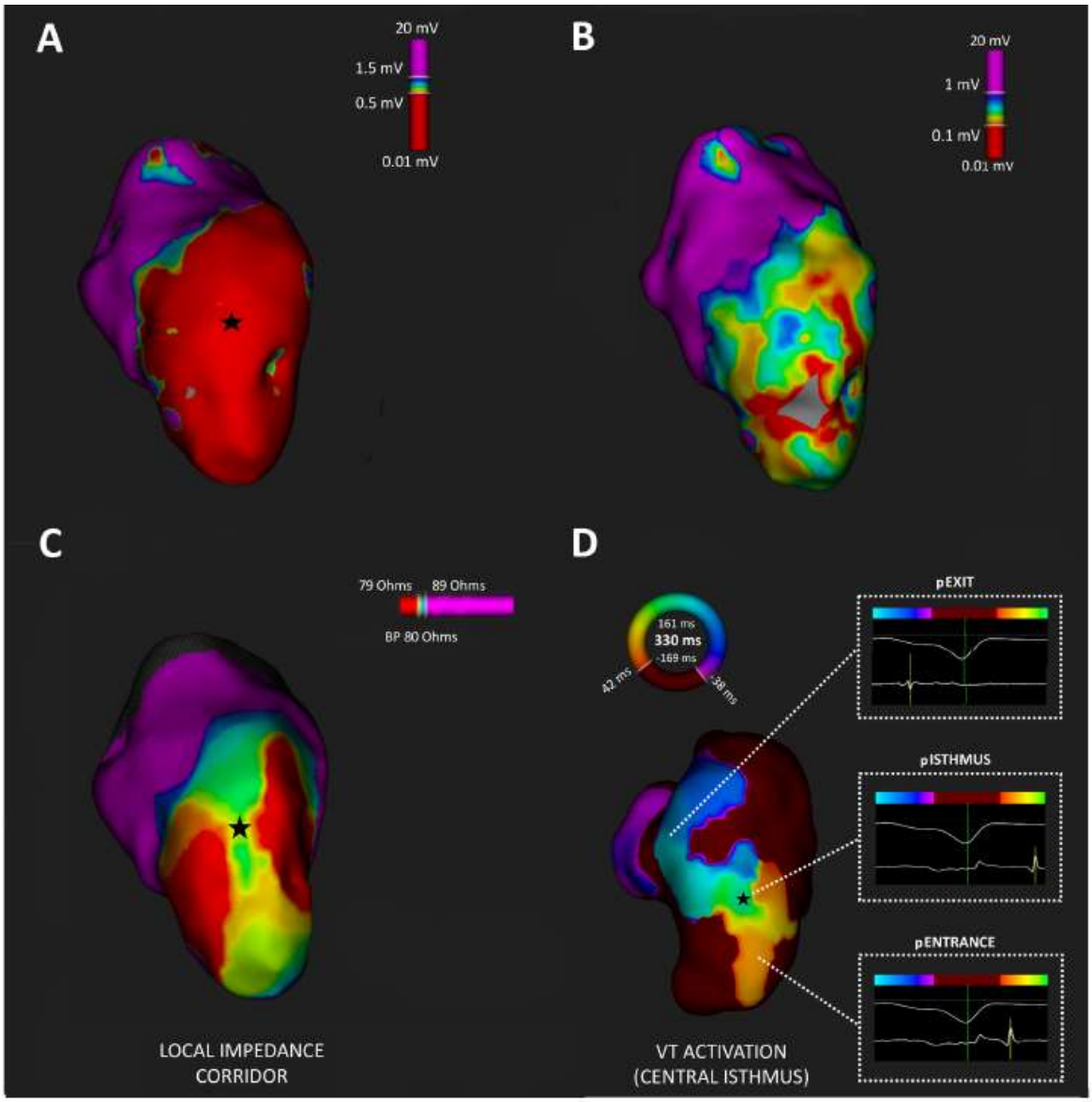
A
20 mV
1.5 mV
0.5 mV
0.01 mV
B
20 mV
1 mV
0.1 mV
0.01 mV
C
79 Ohms
89 Ohms
BP 80 Ohms
LOCAL IMPEDANCE
CORRIDOR
D
161 ms
330 ms
-169 ms
42 ms
-38 ms
pEXIT
pISTHMUS
pENTRANCE
VT ACTIVATION
(CENTRAL ISTHMUS)

Figure 3

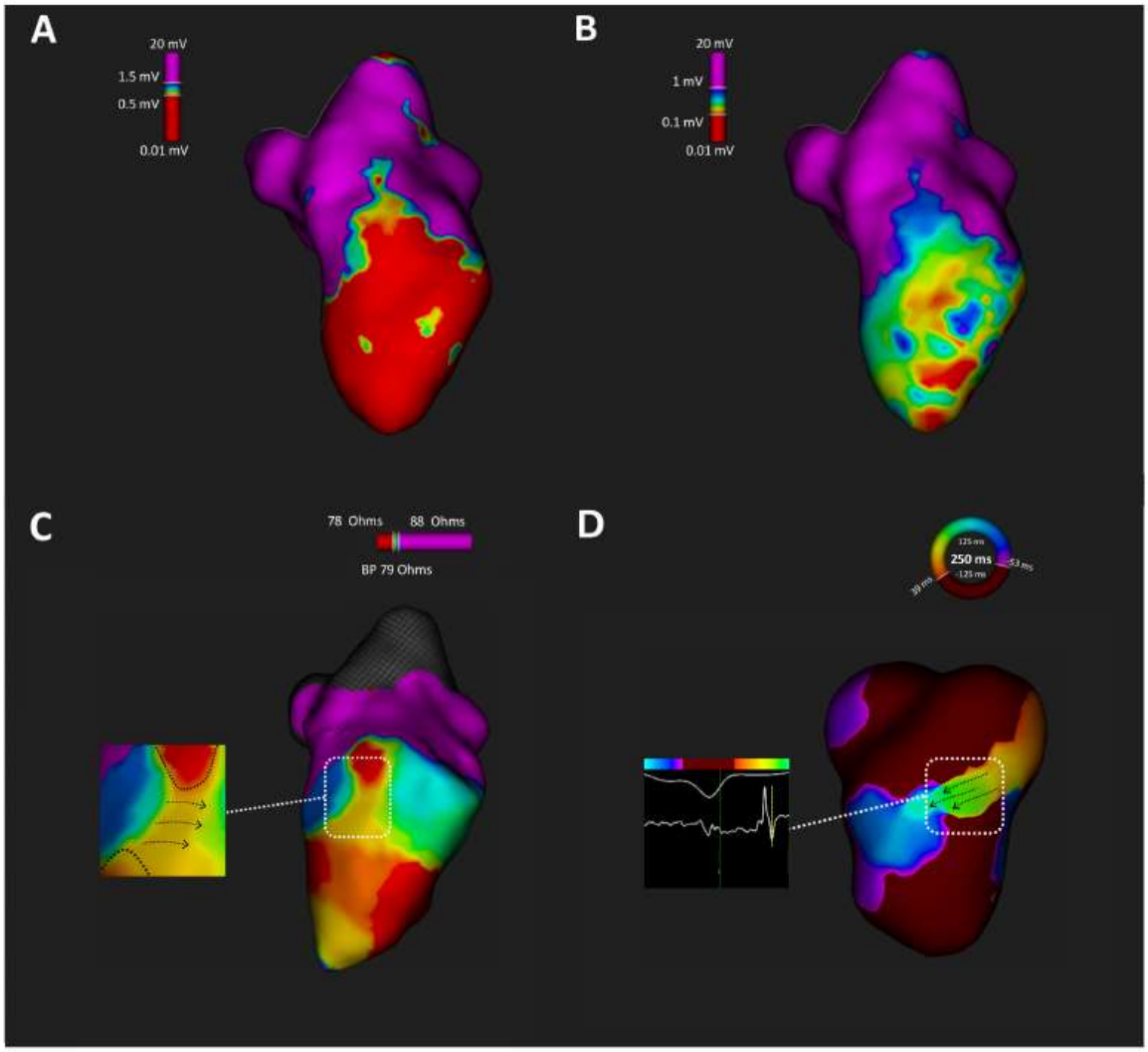
A
20 mV
1.5 mV
0.5 mV
0.01 mV
B
20 mV
1 mV
0.1 mV
0.01 mV
C
78 Ohms
88 Ohms
BP 79 Ohms
D
250 ms

1 **Central Illustration**

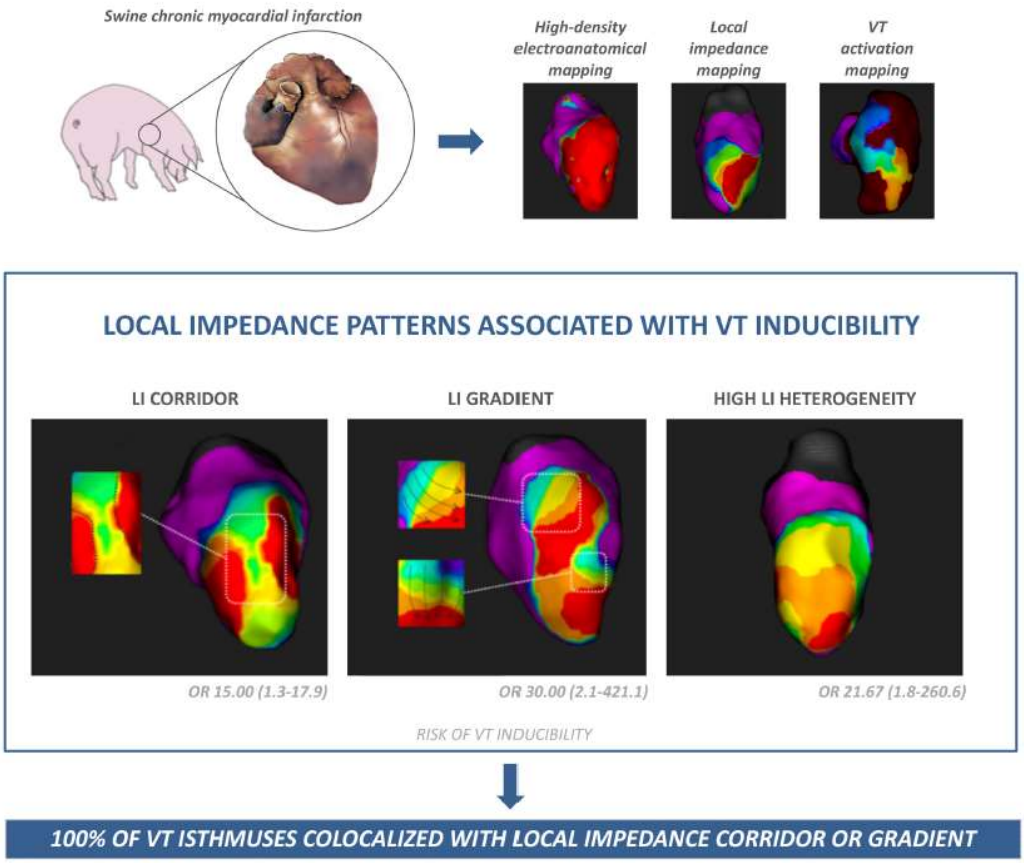

2